

The Mechanism of Increased Vascular Permeability in Renal Ischemic Reperfusion Injury: Potential Role of Angiopietin-1 and Hyaluronan

Adis Tasanarong MD*,***,
Sookkasem Khositseth MD**, Supachai Thitiarchakul MD*

*Nephrology Unit, Department of Medicine, Faculty of Medicine, Thammasat University (Rangsit Campus),
Klong Nung, Klong Luang, Pathumtani, Thailand

**Department of Paediatric, Faculty of Medicine, Thammasat University (Rangsit Campus),
Klong Nung, Klong Luang, Pathumtani, Thailand

***Inter-Department of Biomedical Sciences, Graduate School, Faculty of Medicine,
Chulalongkorn University, Bangkok, Thailand

Background: One striking feature observed during renal ischemia reperfusion injury (IRI) is the increase in interstitial fluid and infiltration, which reflects an increase in vascular permeability. Angiopietin-1 (Ang-1) prevents vascular leakage and inflammation. Hyaluronic acid (HA) has a high capacity to bind and retain water and is pro-inflammatory factor.

Material and Method: The authors evaluated the expression of Ang-1 and HA during renal IRI bilaterally for 30 minutes. Renal tissue was sent for pathologic study, proteins expression, and mRNA in renal IRI at 24 and 48 hr.

Results: At 24 hr post-injury, histopathology studies revealed severe tubular epithelial cell (TEC) necrosis, peritubular capillary (PTC) congestion, mild interstitial infiltration, and edema. Histopathology at 48 hr post-injury showed a progressive increased degree of PTC congestion, interstitial infiltration and edema. In normal kidney, Ang-1 was abundant in glomerulus and PTC patterns, while HA is absent in the cortex but present in the medulla. At 24 and 48 hr post-IRI, kidney cortex and medulla showed a reduced Ang-1 staining but with an increase in HA staining. Western blot analysis showed that levels of Ang-1 expression decreased to 44% of normal levels at 24 hr post-IRI and further declined to 31% at 48 hr post-IRI. Using real time RT-PCR, Ang-1 expression declined to 15% of normal levels at 24 hr post-IRI and sustained at 48 hr post-IRI.

Conclusion: These results suggest that lowered Ang-1 expression levels and increased HA may contribute to an increased permeability and inflammation of microcirculation in renal IRI.

Keywords: Angiopietin-1, Hyaluronic acid, Ischemia, Kidney diseases, Reperfusion injury

J Med Assoc Thai 2009; 92 (9): 1150-8

Full text. e-Journal: <http://www.mat.or.th/journal>

The development of acute renal failure (ARF) is a serious disease causing rapid loss of kidney function, with ARF patients having a high mortality rate. The pathophysiology of ischemic reperfusion induced ARF is a complex interplay between tubular

injury and altered renal microvascular function⁽¹⁾. Functional consequences of these morphological alterations include increased vascular permeability, progression of inflammatory process and imbalanced intravascular hemostatic mechanisms. Accordingly, continued research into the understanding of ARF pathophysiology may facilitate potentially new and improved clinical treatments for the disease.

Normal blood vessels are composed of two distinct cell types: endothelial cell (EC) and mural cells.

Correspondence to: Tasanarong A, Nephrology Unit, Department of Medicine, Faculty of Medicine, Thammasat University (Rangsit Campus), Klong Nung, Klong Luang, Pathumtani 12121, Thailand. Phone: 0-2926-9793, Fax: 0-2926-9793. E-mail: adis_tasanarong@hotmail.com

The mural cell component is comprised of pericytes in capillaries and smaller vessels, whereas larger vessels are built from smooth muscle cell (SMC). Angiopoietin-1 (Ang-1) is a vasculogenic factor that induces EC sprouting, migration, and network formation in the development of new blood vessels⁽²⁾. Ang-1 signaling through Tie 2 is an anti-vascular permeability factor. Vessels growing in the presence of Ang-1 are not leaky due to markedly enhanced pericyte coating of the nascent vessels⁽³⁾. Ang-1 suppresses activation of EC as evidenced by its inhibition of adhesion molecules expression. These effects confer on Ang-1 potent anti-inflammatory properties. Activation of the vascular EC occurs in many clinical scenarios such as inflammatory and reperfusion injury. Under these conditions, EC activation is primarily induced by cytokines such as tumor necrosis factor (TNF- α), interleukin-1 and vascular endothelial growth factor (VEGF) that upregulate many cytokines, chemokines, and adhesion molecules. Activated EC is compromised in its structural and functional integrity, leading to plasma leakage and transmigration of leukocytes into the vessel wall.

Hyaluronic acid (HA) is an important component of the extracellular matrix. It is composed of endless linear repeats of the disaccharide unit. HA biosynthesis is regulated by many pro-inflammatory cytokines. In the kidney, HA is not present in the cortex of the adult kidney, but it is found in the medullary and papillary interstitium, where it plays role in the urinary concentrating process⁽⁴⁾. In contrast, accumulation of HA occurs in various interstitial and glomerular diseases, including ischemic injury⁽⁵⁾, and allograft rejection. Increased accumulation of fluid in interstitial area is a consequence of HA accumulation.

In the present study, the authors investigated the relationship between Ang-1 and HA with the pathological status of renal ischemic reperfusion injury (IRI). This work was conducted in order to gain further insight into the microvascular injury that occurs during IRI. Indeed, the prevention or amelioration of this injury now appears to be an increasingly important component in multipoint therapeutic approaches to the clinical treatment of ARF.

Material and Method

Animals

An official ethics committee in Thammasat University approved all experiments on animals. Male mice weighing 25-30 g were obtained from the National Laboratory Animal Center (Mahidol University) and allowed to acclimatize for 2 weeks prior to surgery.

All mice received tap water and a standard diet and were housed in 12 hr light and 12 hr dark cycle.

Bilateral renal ischemia reperfusion model

All animal experimentation was conducted in accord with the Thammasat Animal Experimental Unit Guideline. Mice were anesthetized with pentobarbital sodium at dose of 35-60 mg/kg by intra-peritoneal injections. The abdominal region was shaved, and the animals were placed on a heating table to maintain them at constant body temperature at $37 \pm 1^\circ\text{C}$ while under anesthesia. The abdomen was soaked with Betadine, and sterile drapes were applied. An abdominal incision was made, and both kidneys were identified. The renal pedicles were clearly dissected and non-traumatic vascular clamp (Roboz Surgical Instrument, Washington, D.C.) was applied across the pedicles bilaterally for 30 min. After the clamps were released, the animals received 3 to 4 ml warm saline via the peritoneal cavity. The wounds were closed in two layers with 4-0 silk and mice were allowed to recover. Following surgery, the animals were returned to the cages, where they had free access to food and water. Thirty-one mice were divided into the following four experimental groups: (1) IRI group in which control mice underwent renal ischemia for 30 minutes followed by reperfusion for 24 hr (n = 8); (2) IRI group in which control mice underwent renal ischemia for 30 minutes followed by reperfusion for 48 hr (n = 8); (3) and (4) control groups for sham operated mice (n = 15), which were subjected to the surgical procedures described above except for the occlusion of the renal arteries. The kidneys from each group of mice were removed after 24 or 48 hr of reperfusion.

At 24 and 48 hr post-ischemia, kidneys were dissected from mice and sliced from the corona. These sections were fixed in 10% formalin and processed for histology using standard techniques. A small section of the kidney was frozen in liquid nitrogen stored at -70°C for protein measurements by Western blot analysis, while another section was fixed in RNAlater Stabilization Solution (Ambion, Inc) for RT-PCR gene expression studies.

Assessment of post ischemic renal function

Blood samples were obtained from the tail vein at 0, 24, and 48 hr post-ischemia and reperfusion. Renal function was assessed by measurement of serum blood urea nitrogen (BUN) and creatinine (Cr) using a Dimension RxL Clinical Chemistry Analyzer (Dade Behring, Inc).

Renal histology

At 24 and 48 hr post-ischemia, kidneys were dissected from mice and tissue slices were fixed in 10% formalin and processed for histology examination using standard techniques. Formalin tissue was embedded in paraffin and 4-micrometer sections were stained with hematoxylin and eosin (H&E) and periodic acid-Schiff (PAS). These sections were examined in a blinded fashion by a nephrologist. The percentage of histology changes, such as degree of tubular epithelial cell (TEC) necrosis, peritubular capillary (PTC) congestion, interstitial edema and infiltration were evaluated under high power magnification (400x) in 5 to 10 consecutive fields, and mean percentages of histological change were then calculated.

Reagents

Reagents were obtained from Sigma-Aldrich (Capricorn, Singapore Science Park II, Singapore) unless specified otherwise. Rabbit anti-mouse Ang-1 antibody was from Alpha Diagnostic International (San Antonio, TX), and hyaluronidase was from BDH Inc. (Thailand).

Immunohistochemical analyses

Organs were fixed in 4% paraformaldehyde. Five-micrometer paraffin sections were dewaxed and rehydrated. For antigen retrieval, kidney sections were incubated with proteinase K for 6 min. Endogenous peroxidase was quenched with 3% H₂O₂ for 20 min, and non-specific binding blocked with 20% normal goat serum in phosphate-buffered saline (PBS) (pH 7.4). Sections were treated with anti-Ang-1 antibody (1:500) for 1 hr followed by Envision reagent (Dako, Bangkok Thailand) containing anti-rabbit secondary antibodies for 30 min, and finally with 3,5-diaminobenzidine (DAB) substrate for 10 min. Negative controls using normal rabbit IgG were also included. Nuclei were counterstained with hematoxylin for 2 min, and slides were dehydrated and mounted with permount.

Alcian blue staining

Alcian blue stain was used to visualize HA (glycoaminoglycan). Briefly, 5-micrometer paraffin section slides were deparaffinized, rehydrated, and incubated in 3% acetic acid solution for 5 minutes. The slides were then incubated with 2% Alcian blue, pH 2.5, at 37°C for 15 minutes. The slides were washed in distilled water, followed by counterstaining with Nuclear Fast Red solution for 5 minutes and mounted with permount.

Hyaluronidase digestion method

Hyaluronidase treatment of tissues was performed by incubating tissue sections with 0.025 g bovine testicular hyaluronidase in 50 ml of PBS for 3 h at 37°C. The sections were stained with Alcian blue as described above. The hyaluronidase digestion experiments also included negative controls lacking the enzyme.

Protein extraction

Briefly, 40 mg of kidney (wet weight) was homogenized in 240 µl of 40 mM Tris-HCl (pH 7.6) buffer containing 0.1% Nodinet P-40, 0.05% sodium deoxycholate, 0.01% SDS, 150 mM NaCl, and 10 mM 2-mercaptoethanol. Homogenates were treated with 60 µg/ml of PMSF and centrifuged in a pre-chilled rotor at 15,000xg for 15 min. Supernatants were stored at -70°C. Protein content was measured using a BCA™ Protein Assay Kit (PIERCE, IL, USA)

Western blot

Protein samples were electrophoresed on 12% SDS-PAGE mini-gels and wet-transferred (Bio-Rad, ON, Canada) onto nitrocellulose membranes. Membranes were treated with blocking solution followed by an overnight incubation at 4°C with anti-Ang-1 polyclonal antibody (Alpha diagnostic, TX, USA) diluted to 1:500 in 5% BSA-TTBS. The secondary antibody (PIERCE, IL, USA) was diluted to 1:100,000 in 5% BSA-TTBS and membranes treated for 1 hour at room temperature. Signals were visualized by chemiluminescent detection according to the manufacturers' instructions (PIERCE, IL, USA). Signals were quantified using GeneGnome Syngene Bio Imagine and GeneSnap image acquisition software (Syngene, MD, USA).

Real time RT-PCR

Total RNA were extracted using the RNeasy mini kit (Qiagen, Chatworth, CA, USA) according to the manufacturers' instructions. High-quality RNA was eluted in 35 µl RNase-free water. An aliquot of each RNA preparation was used to determine total RNA quality and concentration, measured at 260 nm (OD₂₆₀). Pure RNA possessed an OD₂₆₀/OD₂₈₀ ratio of 1.6-1.9. Total RNA (0.25 µg) was reverse-transcribed to cDNA by Taqman Reverse Transcriptase Reagent (Applied Biosystems, Roch Molecular Biochemical, NJ, USA) using random primers using the following cycling conditions: 25°C, 10 min; 48°C, 30 min; 95°C, 5 min.

The mRNA levels of Ang-1 and hypoxanthine phosphoribosyltransferase (HPRT) were measured

using a LightCycler® machine (Roche Molecular Biochemicals, Indianapolis, IN, USA) with the TaqMan probe. Table 1 contains the sequences of primers and fluorescence probes for Ang-1 and HPRT. The probes were labeled with 6-carboxy-fluorescein (FAM) at the 5' end, and with 6-carboxytetramethylrodamine (TAMRA) at the 3' end. FAM served as the reporter dye, and TAMRA serves as the quencher dye. All primer pairs were designed to span across intron-exon boundaries in order to test for any genomic DNA contamination of RNA samples. Each PCR was assembled in 20 ml volumes consisting of 10 ml of 2 x QuantiTech Probe mastermix (Qiagen, Chatworth, CA, USA), 0.5 ml of 20 mM forward primer, 0.5 ml of 20 mM reverse primer, 0.2 ml of 20 mM probe and 6.8 ml of RNase-free water. Following the addition of 2 ml of cDNA template, PCR amplification was performed using an initial denaturation step at 95°C for 15 minutes, then 50 cycles of heating at 95°C and immediate cooling to 58°C (for Ang-1) or 55°C (for HPRT) for 60 seconds. Real-time PCR results were automatically recorded by LightCycler® software (version 4.05) and analyzed by relative quantification using the comparative Ct method.

Statistical analyses

Data were expressed as mean \pm SD. Statistical analyses were carried out using the SPSS software (version 12.0). Statistically significant differences among groups were calculated by ANOVA Bonferroni and Mann-Whitney tests using the least significant difference method. Statistical significances were defined as $p < 0.05$.

Results

Changes in serum creatinine during renal ischemic reperfusion injury

Ischemia-induced renal dysfunction was assessed at 24 and 48 hr following post-ischemic

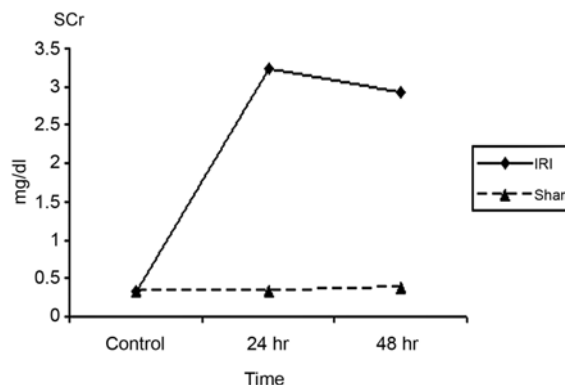


Fig. 1 Renal function as assessed by measurement of serum creatinine in mouse renal ischemic reperfusion injury

reperfusion. Severe ARF was observed, showing functional impairment at both time points. In wild-type mice subjected to bilateral renal pedicle clamping for 30 min, SCr levels (mg/dl) increased from 0.32 ± 0.08 to 3.23 ± 0.55 after 24 hr of reperfusion and remained elevated at 2.93 ± 0.15 at 48 hr (Fig. 1). However, SCr levels were not different in sham groups at both 24 and 48 hr compared with the control group.

Changes in organ weight and histology during renal ischemic reperfusion injury

Renal IRI were studied in all four groups of mice. Organ weights and the histopathological assessments of renal IRI and control kidneys are shown in Table 2. The mean kidney weight in 24 hr post-IRI group increased to 109% while in 48 hr post-IRI group it increased further to 115% when compared to the sham (control) group. IRI lesions were evaluated at 24 and 48 hr post-IRI, compared to sham kidneys (Table 2 and Fig. 2A-F). At 24 h after IRI, up to 90% of the proximal tubular cells in the outer stripe of outer

Table 1. Sequences of real-time PCR primers and probes

Gene		Sequence
Ang-1	Forward	5'-GGACACCTTGAAGGAGGAGAAAG-3'
	Reverse	5'-TTCTCCAACCTCTGGATGATGA-3'
	Probe	5'-FAM-CCTTCAAGGCTTGGTTTCTCGTCAGACA-TAMRA-3'
HPRT	Forward	5'-TGACACTGGTAAAACAATGCAAACT-3'
	Reverse	5'-AACAAAGTCTGGCCTGTATCCAA-3'
	Probe	5'-TTCACCAGCAAGCTTGCAACCTTAACC-3'

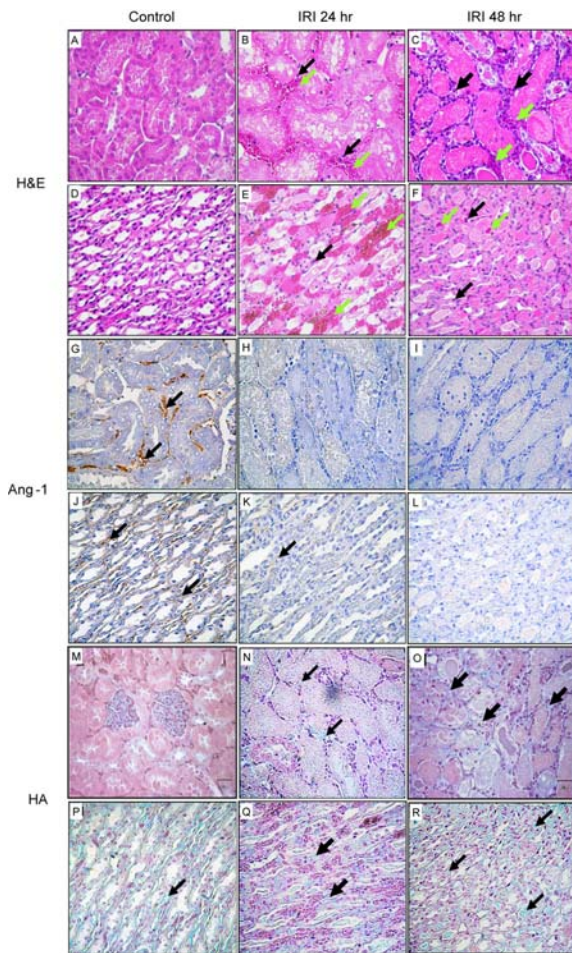


Fig. 2 Histology and immunohistological staining of mouse renal IRI. (A) and (D). Normal mouse kidney in cortex and medulla (H&E). (B) and (E). At 24 hr post IRI shows severe TEC necrosis, PTC congestion (green arrows), mild interstitial infiltration and edema (black arrows) in cortex and medulla. (C) and (F). At 48 hr post IRI shows progressively increased degrees of PTC congestion (green arrows), interstitial infiltration and edema (black arrows) in cortex and medulla. (G) and (J). Ang-1 in normal kidney shows strong staining in the PTC pattern in cortex and medulla (black arrows). (H) and (K). Decreased Ang-1 staining in the PTC pattern in cortex and medulla at 24 hr post IRI. (I) and (L). Progressive loss of Ang-1 staining in the PTC pattern in cortex and medulla at 48 hr post IRI. (M) and (P). Alcian blue staining in normal kidney shows no staining in renal cortex but prominent staining in medulla. (N) and (Q). At 24 hr post IRI shows increased HA staining (black arrows) in the interstitial area of renal cortex and medulla. (O) and (R). Progressive increased of HA staining (black arrows) in the interstitial area of renal cortex and medulla. Magnifications: x400 in A-R

Ang-1 protein expression in IRI time course

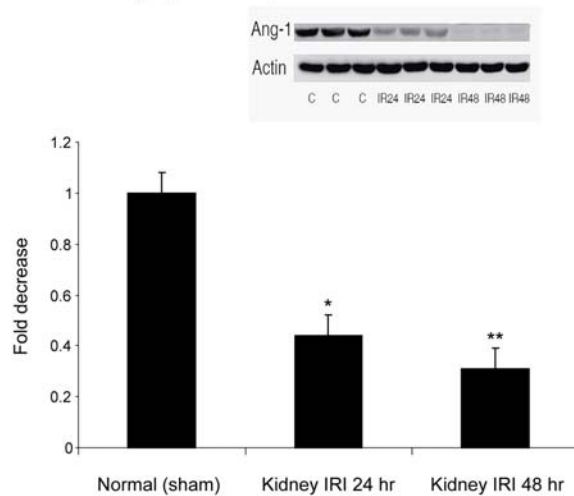


Fig. 3 Ang-1 protein expression by western blot analysis during the time course of renal IRI. Fold decrease was calculated from the ratio of band intensities in control (C) and renal IRI (IR). Each bar represents the mean \pm SD of three experiments. * Significant differences compared to normal kidneys by ANOVA Bonferroni tests, $p < 0.05$. ** Significant differences compared to normal kidneys by ANOVA Bonferroni tests, $p < 0.01$.

Ang-1 gene expression in IRI time course

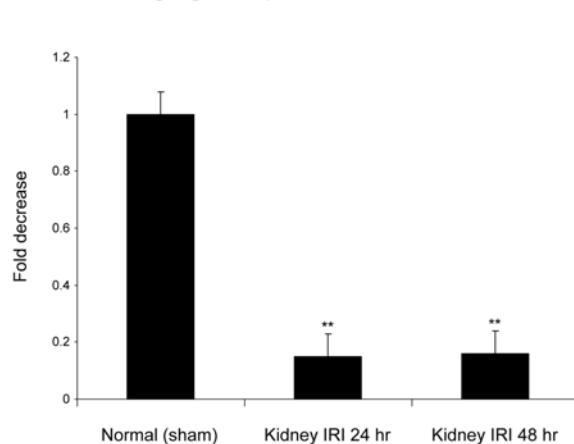


Fig. 4 Ang-1 mRNA expression by real time RT-PCR during the time course of renal IRI. Each bar represents the mean \pm SD of three experiments. ** Significant differences compared to normal kidneys by ANOVA Bonferroni tests, $p < 0.01$.

Table 2. Histopathology in mouse renal ischemic reperfusion injury

Subject	Normal (sham)	Kidney IRI 24 hr	Kidney IRI 48 hr
Weight (mg)	590.0 ± 21.9	645.0 ± 18.7*	680.0 ± 40.5*
Tubular epithelial cell necrosis (%)	0.0	96.4 ± 2.3*	97.1 ± 2.0*
PTC congestion (%)	0.0	8.7 ± 1.3*	19.2 ± 1.2*
Interstitial edema (%)	0.0	8.9 ± 1.0*	19.5 ± 1.4*
Interstitial infiltration (%)	0.0	5.3 ± 1.6*	18.9 ± 1.7*

The percentage of weight and histopathology changes, such as degree of tubular epithelial cell necrosis, PTC congestion, interstitial edema and infiltration

Values are means ± SD

* Significant difference compared to sham group by Mann-Whitney test ($p < 0.05$)

medulla (OSOM) and cortex were severely damaged. Such damage included the widespread loss of brush border and cellular nuclei, a denudation of tubular cells, tubular dilatation, and sloughing of proximal tubules with obstructing granular casts. This contrasted markedly to the sham control kidney samples. In clamped kidney tissue after 24 hours, PTC congestion and interstitial edema were observed in the OSOM and cortex. Infiltration of polymorphonuclear and mononuclear cell was observed in the interstitium of the renal parenchyma, primarily around the PTC, which was most severe after 48 hours. However, no histopathological changes were observed at any time in the sham mice renal tissue samples.

Expression of angiotensin-1 in renal IRI

The authors examined the localization and expression of Ang-1 during the time course of renal IRI. In sham kidneys, Ang-1 was detected in all glomeruli and PTC patterns (Fig. 2G-J). However, Ang-1 staining in glomerulus and PTC was decreased at 24 hr post-IRI in cortex and medulla (Fig. 2H-K) and further decreases were observed at 48 hr (Fig. 2I-L). Lower abundances of Ang-1 protein during renal IRI were also confirmed, using Western blots (Fig. 3). Expression of the glycosylated form of Ang-1 (90 kDA) declined to 44% at 24 hr post-IRI and 31% at 48 hr post-IRI. Furthermore, Ang-1 mRNA levels were assessed using real time RT-PCR (Fig. 4), which showed that Ang-1 mRNA expression decreased to 15% at 24 hr post-IRI and 16% at 48 hr post-IRI when compared to sham kidney RNA samples.

Elevated hyaluronic acid in renal IRI

The authors studied the changes in renal HA content in renal IRI by Alcian blue staining. In normal

(sham) mice kidney, HA staining was localized in the medulla area, and could not be detected in the cortex (Fig. 2M-P). Kidneys in IRI group demonstrated interstitial HA at 24 hr post-IRI in both cortex and medulla (Fig. 2N-2Q) with progressive increased staining at 48 hr post-IRI (Fig. 2O-R).

Discussion

In the present report, the authors have evaluated some of the important factors known to be associated with the vascular permeability and inflammation in mice renal IRI. The authors observed renal weight gain, PTC congestion, interstitial edema, and infiltration at 24 hr post-IRI, and by 48 hr post-IRI, kidney weight, PTC congestion, interstitial edema, and infiltration were further elevated. There was also a concomitant decrease in both Ang-1 mRNA and protein expression, and increase HA accumulation while PTC congestion, interstitial edema, and infiltration continued to worsen. Therefore, a relationship between decreased Ang-1 expression, increased HA accumulation and vascular leakage and inflammation was confirmed in the present study.

Progressive decreases in Ang-1 and increases in HA accumulation during renal IRI is a novel observation. Loss of the anti-permeability effects of Ang-1 and increased water binding capacity by HA synthesis is associated with the degree of PTC congestion and interstitial edema in renal IRI. VEGF is a potent multifunctional cytokine that promotes angiogenesis, and increases vascular permeability. VEGF is produced by podocytes in glomeruli and TEC in the kidney. However, previous studies have demonstrated that renal IRI does not lead to increased VEGF expression^(6,7). Ang-1 is another potent cytokine produced by podocytes in glomeruli⁽⁸⁾, pericytes and

SMC in blood vessels⁽⁹⁾. It binds to the Tie-2 receptor on EC and provides signals that promote EC function, survival, and prevents plasma leakage⁽³⁾. During inflammation, some pericytes can act like APC in indirect pathways by increasing MHC class I and II molecule expression after stimulation by many cytokines, and to present antigen to the T lymphocyte stimulated immune response⁽¹⁰⁾. Upregulation of VCAM expression on SMC and SMC phenotypic change was mediated by MHC molecules and many cytokines⁽¹¹⁾. Both pericytes and SMC are targets of T lymphocyte functional changes and/or damage. Therefore, injury to pericytes and SMC contributing to decrease Ang-1 production may cause EC dysfunction, thereby promoting increased vascular permeability and leakage.

In the normal kidney, HA is detected only in the interstitium of the renal inner medulla, in contrast to the low amounts seen in other regions of the kidney as seen in the present study. HA in the inner medulla is produced by specialized type 1 interstitial cells that play a role to concentrate solutes in the inner medulla. In both *in vitro* and *in vivo* studies, up regulation of HAS2 gene expression and increase HA production were observed in EC⁽¹²⁾ and SMC⁽¹³⁾. During kidney injury, up regulation of HAS2 gene expression and enhanced HA synthesis occurs in the glomeruli and TEC⁽¹⁴⁾. HAS2 gene expression is highly upregulated during renal IRI⁽¹⁵⁾, along with an accumulation of HA in the interstitial area in the renal medulla and renal cortex as detected by alcian blue staining. HA accumulation in this area affords a high water-binding capacity with the fluid that leaks from PTC in interstitial edema. Leakage of plasma from the intravascular space through EC caused from a loss of Ang-1 contributes to a hemoconcentration, leading to stasis and impaired perfusion in the corticomedullary junction. Hemoconcentration and stasis also increase the potential for EC-leukocyte interactions. Congestion of the renal microcirculation especially in the PTC of the outer medullary region contributes to deficits in renal perfusion. Thus, hemoconcentration, vascular congestion, and edema formation cause impaired renal perfusion inducing loss of renal function.

Loss of the anti-inflammatory effect of Ang-1 and an increased pro-inflammatory effect of HA synthesis is associated with the degree of interstitial infiltration in renal IRI. These effects should result from severe loss of a nuclear factor- κ B (NF- κ B) inhibitory effect of Ang-1, and activated NF- κ B by HA promotes expression of adhesion molecules on EC for leukocyte

extravasations. In renal IRI, many cytokines induce the upregulation of chemokines and cell adhesion molecule genes by the NF- κ B regulatory system on EC⁽¹⁶⁾. However, it was reported that TGF-beta could negatively regulate Ang-1 expression in SMC⁽¹⁷⁾. TGF-beta, a pro-fibrotic cytokine, is produced in large quantities by kidney epithelium, and invading T cells during rejection can decrease Ang-1 expression. Ang-1 is a powerful inhibitor of VEGF in terms of anti-inflammation. Recent studies demonstrated that Ang-1 can reduce ICAM-1, VCAM-1, and E-selectin expression and inflammation counteracts VEGF activity⁽¹⁸⁾ through the Tie2 receptor by acting as a NF- κ B inhibitor⁽¹⁹⁾. The A20 binding inhibitor of NF- κ B activation-2 (ABIN-2) was found to inhibit EC apoptosis and rescue cells from death through Ang-1⁽²⁰⁾. Studies in proximal TEC culture demonstrated that the activation of NF- κ B is associated with the synthesis of HA by transcriptional activation of HAS2⁽¹⁴⁾. The major HA receptor is CD44 is only found on interstitial dendritic cells and passenger leukocytes in normal kidney. In contrast, CD44 is markedly enhanced in inflammatory renal diseases, particularly on TEC and T lymphocyte during inflammation⁽²¹⁾. CD44 on lymphocytes bind with HA on the EC surface, which can mediate primary adhesion (rolling interactions) of lymphocytes on vascular EC. This adhesion pathway is utilized in the extravasation of activated T cells from the blood into sites of inflammation. After the activation of CD44 expression, T lymphocyte binds with HA accumulation in interstitial area, leading to different degrees of interstitial infiltration in renal IRI.

The authors postulate that the concomitant and reciprocal changes in Ang-1 and HA expression have important implications for renal IRI. Both factors are controlled by the intra-renal inflammatory cytokines and chemokines as cross-talk between microcirculation with TEC, which may be a part of T cell mediated injury during the development of interstitial edema and infiltration.

Acknowledgments

The study was supported by a grant from the Thailand Research Fund. The authors wish to thank Professor Sittichai Koonthongkaew for his help with the western blots.

References

1. Bonventre JV, Weinberg JM. Recent advances in the pathophysiology of ischemic acute renal failure. *J Am Soc Nephrol* 2003; 14: 2199-210.

2. Hayes AJ, Huang WQ, Mallah J, Yang D, Lippman ME, Li LY. Angiopoietin-1 and its receptor Tie-2 participate in the regulation of capillary-like tubule formation and survival of endothelial cells. *Microvasc Res* 1999; 58: 224-37.
3. Thurston G, Rudge JS, Ioffe E, Zhou H, Ross L, Croll SD, et al. Angiopoietin-1 protects the adult vasculature against plasma leakage. *Nat Med* 2000; 6: 460-3.
4. MacPhee PJ. Estimating rat renal medullary interstitial oncotic pressures and the driving force for fluid uptake into ascending vasa recta. *J Physiol* 1998; 506 (Pt 2): 529-38.
5. Johnsson C, Tufveson G, Wahlberg J, Hallgren R. Experimentally-induced warm renal ischemia induces cortical accumulation of hyaluronan in the kidney. *Kidney Int* 1996; 50: 1224-9.
6. Kanellis J, Mudge SJ, Fraser S, Katerelos M, Power DA. Redistribution of cytoplasmic VEGF to the basolateral aspect of renal tubular cells in ischemia-reperfusion injury. *Kidney Int* 2000; 57: 2445-56.
7. Kanellis J, Paizis K, Cox AJ, Stacker SA, Gilbert RE, Cooper ME, et al. Renal ischemia-reperfusion increases endothelial VEGFR-2 without increasing VEGF or VEGFR-1 expression. *Kidney Int* 2002; 61: 1696-706.
8. Satchell SC, Harper SJ, Tooke JE, Kerjaschki D, Saleem MA, Mathieson PW. Human podocytes express angiopoietin 1, a potential regulator of glomerular vascular endothelial growth factor. *J Am Soc Nephrol* 2002; 13: 544-50.
9. Davis S, Aldrich TH, Jones PF, Acheson A, Compton DL, Jain V, et al. Isolation of angiopoietin-1, a ligand for the TIE2 receptor, by secretion-trap expression cloning. *Cell* 1996; 87: 1161-9.
10. Balabanov R, Beaumont T, Dore-Duffy P. Role of central nervous system microvascular pericytes in activation of antigen-primed splenic T-lymphocytes. *J Neurosci Res* 1999; 55: 578-87.
11. Reed EF. Signal transduction via MHC class I molecules in endothelial and smooth muscle cells. *Crit Rev Immunol* 2003; 23: 109-28.
12. Estess P, Nandi A, Mohamadzadeh M, Siegelman MH. Interleukin 15 induces endothelial hyaluronan expression in vitro and promotes activated T cell extravasation through a CD44-dependent pathway in vivo. *J Exp Med* 1999; 190: 9-19.
13. Pullen M, Thomas K, Wu H, Nambi P. Stimulation of Hyaluronan synthetase by platelet-derived growth factor bb in human prostate smooth muscle cells. *Pharmacology* 2001; 62: 103-6.
14. Jones S, Jones S, Phillips AO. Regulation of renal proximal tubular epithelial cell hyaluronan generation: implications for diabetic nephropathy. *Kidney Int* 2001; 59: 1739-49.
15. Goransson V, Johnsson C, Jacobson A, Heldin P, Hallgren R, Hansell P. Renal hyaluronan accumulation and hyaluronan synthase expression after ischaemia-reperfusion injury in the rat. *Nephrol Dial Transplant* 2004; 19: 823-30.
16. Read MA, Whitley MZ, Williams AJ, Collins T. NF-kappa B and I kappa B alpha: an inducible regulatory system in endothelial activation. *J Exp Med* 1994; 179: 503-12.
17. Nishishita T, Lin PC. Angiopoietin 1, PDGF-B, and TGF-beta gene regulation in endothelial cell and smooth muscle cell interaction. *J Cell Biochem* 2004; 91: 584-93.
18. Kim I, Moon SO, Park SK, Chae SW, Koh GY. Angiopoietin-1 reduces VEGF-stimulated leukocyte adhesion to endothelial cells by reducing ICAM-1, VCAM-1, and E-selectin expression. *Circ Res* 2001; 89: 477-9.
19. Hughes DP, Marron MB, Brindle NP. The anti-inflammatory endothelial tyrosine kinase Tie2 interacts with a novel nuclear factor-kappaB inhibitor ABIN-2. *Circ Res* 2003; 92: 630-6.
20. Tadros A, Hughes DP, Dunmore BJ, Brindle NP. ABIN-2 protects endothelial cells from death and has a role in the antiapoptotic effect of angiopoietin-1. *Blood* 2003; 102: 4407-9.
21. DeGrendele HC, Kosfisz M, Estess P, Siegelman MH. CD44 activation and associated primary adhesion is inducible via T cell receptor stimulation. *J Immunol* 1997; 159: 2549-53.

กลไกการเพิ่มขึ้นของ vascular permeability ในไตที่ได้รับบาดเจ็บภายหลังจากการขาดเลือด และได้รับเลือดกลับคืนมาหลอเลียง: ผลของ angiotensin-1 และ hyaluronan

อดิศว์ ทัศนรงค์, สุขเกษม โฆษิตเศรษฐ, ศุภชัย จิตติอาชากุล

ภูมิหลัง: พยาธิสภาพที่สำคัญอย่างหนึ่งของไตที่ได้รับบาดเจ็บภายหลังจากการขาดเลือด และได้รับเลือดกลับคืนมาหลอเลียง คือ การตรวจพบของเหลว และเซลล์การอักเสบในบริเวณ interstitium ซึ่งบ่งบอกถึง การเพิ่มขึ้นของ vascular permeability จากการศึกษาพบว่า angiotensin-1 (Ang-1) สามารถป้องกัน vascular leakage และขบวนการอักเสบได้ ส่วน hyaluronic acid (HA) มีความสามารถในการอุ้มน้ำ และกระตุ้นขบวนการอักเสบ

วัสดุและวิธีการ: การศึกษานี้จึงได้ออกแบบมาเพื่อดูการเปลี่ยนแปลงของ Ang-1 และ HA ในไตหนูทั้งสองข้างที่ได้รับบาดเจ็บภายหลังจากการขาดเลือดเป็นเวลา 30 นาที และได้รับเลือดกลับคืนมาหลอเลียง

ผลการศึกษา: จากการศึกษาพบว่า ณ เวลา 24 ชั่วโมงหลังการบาดเจ็บ พบว่ามีการถูกทำลายของเซลล์ท่อไตอย่างรุนแรง, หลอดเลือดแดงเล็กที่อยู่รอบ ๆ ท่อไตมีการขยายตัวและมีเม็ดเลือดแดงคั่งอยู่เป็นจำนวนมาก, พบการบวม และเซลล์อักเสบเพิ่มขึ้นเล็กน้อยในบริเวณ interstitium นอกจากนี้ ณ เวลา 48 ชั่วโมง หลังการบาดเจ็บ พบว่าเซลล์ท่อไตยังมีการถูกทำลายอย่างรุนแรง, หลอดเลือดแดงเล็กที่อยู่รอบ ๆ ท่อไตมีการขยายตัว และมีเม็ดเลือดแดงคั่งอยู่เป็นจำนวนมากขึ้น รวมทั้งมีการบวมเพิ่มขึ้น และเซลล์การอักเสบในบริเวณ interstitium มากกว่าที่ 24 ชั่วโมง หลังการบาดเจ็บ ส่วนการย้อม immunohistochemistry พบว่าในไตหนูปกติจะมีการย้อมติด Ang-1 ที่บริเวณ โกลเมอรูลัส และหลอดเลือดแดงเล็กที่อยู่รอบ ๆ ท่อไต ขณะที่จะย้อมไม่พบ HA ในบริเวณ cortex ของไต แต่จะย้อมติดในบริเวณ interstitium ของทั้ง cortex และ medulla ตามลำดับ แต่พบการย้อมติดของ Ang-1 ลดลงอย่างต่อเนื่อง และการลดลงของโปรตีน Ang-1 นี้ได้รับการยืนยันโดยการตรวจ western blot analysis พบการลดลงของโปรตีน Ang-1 เหลือร้อยละ 44 ที่ 24 ชั่วโมง และร้อยละ 31 ที่ 48 ชั่วโมง หลังการบาดเจ็บ รวมทั้งการตรวจจีน Ang-1 โดยวิธี real time RT-PCR พบว่า มีการลดลงของจีน Ang-1 เหลือร้อยละ 15 ที่ 24 ชั่วโมง และยังคงลดลงเท่า ๆ เดิมที่ 48 ชั่วโมง หลังการบาดเจ็บ

สรุป: การลดลงของ Ang-1 และการเพิ่มขึ้นของ HA ในไตหนูที่ได้รับการบาดเจ็บหลังจากการขาดเลือด และได้รับเลือดกลับคืนมาหลอเลียง อาจเป็นสาเหตุหนึ่งที่ทำให้มีการเพิ่มขึ้นของ vascular permeability และทำให้เกิดขบวนการอักเสบในไต
